

# Universality of the Anderson transition with the quasiperiodic kicked rotor

G. LEMARIÉ<sup>1</sup>, B. GRÉMAUD<sup>1,2</sup> and D. DELANDE<sup>1</sup>

<sup>1</sup> *Laboratoire Kastler Brossel, UPMC, ENS, CNRS; 4 Place Jussieu, F-75005 Paris, France*

<sup>2</sup> *Centre for Quantum Technologies, National University of Singapore, 3 Science Drive 2, Singapore 117543, Singapore*

PACS 72.15.Rn – Localization effects (Anderson or weak localization)

PACS 03.75.-b – Matter waves

PACS 71.30.+h – Metal-insulator transitions and other electronic transitions

**Abstract.** - We report a numerical analysis of the Anderson transition in a quantum-chaotic system, the quasiperiodic kicked rotor with three incommensurate frequencies. It is shown that this dynamical system exhibits the same critical phenomena as the truly random 3D-Anderson model. By taking proper account of systematic corrections to one-parameter scaling, the universality of the critical exponent is demonstrated. Our result  $\nu = 1.59 \pm 0.01$  is in perfect agreement with the value found for the Anderson model.

**Introduction.** – It is now widely acknowledged that the classical diffusive behavior of non-interacting electrons in a disordered potential can be stopped by non-trivial interference effects [1]. This puzzling phenomenon, Anderson localization, constitutes one strong evidence of the very difference between quantum and classical dynamics of complex systems. A similar phenomenon is observed in the dynamics of the quantum kicked rotor, a paradigmatic system of quantum chaos: the dynamical localization, where quantum mechanical interference tend to suppress the classical chaotic diffusive dynamics. The discovery of the parallel between dynamical localization and Anderson localization originated from the mapping of the kicked rotor to the quasirandom 1D Anderson model [2]. In Ref. [3] it was demonstrated that the kicked rotor in the dynamical localization regime could be modeled by random band matrices; the latter have been reduced to a 1D non-linear  $\sigma$  model [4] similar to those employed in the localization theory [5]. In Ref. [6] the direct correspondence between the kicked rotor and the diffusive supersymmetric non-linear  $\sigma$  model was demonstrated. In the localized regime, the kicked rotor *exactly* mimics the behavior of disordered electronic conductors.

There has been much experimental efforts to observe Anderson localization in 3D. However, due to stray effects like interaction, decoherence or absorption, very few attempts have been successful [7]. In a slightly different context, Anderson localization of acoustic [8] and electromagnetic [9–12] waves has been experimentally observed.

The experimental realization of the kicked rotor with laser-cooled atoms interacting with a pulsed standing wave allowed for the first experimental observation of Anderson localization in 1D with atomic matter waves [13]. One step further is to observe the well-known Anderson *transition* with this type of system, i.e. the disorder induced metal-insulator transition predicted for non-interacting electrons in a 3D disordered potential. Different generalizations of the kicked rotor have been theoretically considered as analogs of the 3D-Anderson model [14]. Here, we focus on the convenient three-incommensurate-frequencies generalization introduced in Ref. [15]. Very recently an experiment based on this system has fully characterized the Anderson metal-insulator transition [16]: a careful analysis of the scaling properties of the dynamics resulted in the first experimental determination of the localization length critical exponent  $\nu$ . The value found  $\nu = 1.4 \pm 0.3$  is compatible with the precedent numerical determination of  $\nu = 1.57 \pm 0.02$  for the true-random 3D-Anderson model [17].

At this stage, the equivalence between the quasiperiodic kicked rotor [16] and 3D-disordered conductors still has the status of a conjecture (see [18]). A rigorous answer to the question whether this dynamical system exhibits the same critical phenomena –i.e. belongs to the same universality class– as the true 3D-Anderson model has not yet been given. Can a simple three-frequency dynamical system exactly mimic the critical behavior of 3D disordered electronic conductors? In this Letter, we show that the an-

swer is positive. This is done by carrying out a very precise numerical study of the critical behavior of the quasiperiodic kicked rotor *with the same care* as in the most sophisticated investigations of the critical behavior of the true 3D-Anderson model [17, 19, 20]. The fact that both models give the same localization length critical exponent  $\nu$  within comparable (small) uncertainties implies that they belong to the same universality class (orthogonal) [21].

**The quasiperiodic kicked rotor.** – The quasiperiodic kicked rotor we consider is a three-incommensurate-frequencies generalization of the kicked rotor:

$$H_{qp} = \frac{p^2}{2} + \mathcal{K}(t) \cos \theta \sum_n \delta(t - n), \quad (1)$$

obtained simply by modulating the amplitude of the standing wave pulses with a set of two new incommensurate frequencies  $\omega_2$  and  $\omega_3$  of modulation:

$$\mathcal{K}(t) = K [1 + \varepsilon \cos(\omega_2 t + \varphi_2) \cos(\omega_3 t + \varphi_3)]. \quad (2)$$

Here we consider the case with an effective Planck constant  $\hbar = -i[\theta, p]$ . For a standard rotor,  $\theta$  is an angle defined modulo  $2\pi$  and the wavefunction thus has to be  $2\pi$  periodic. In the atomic realization of the kicked rotor [16], the Hamiltonian is still given by Eq. (1), with  $\theta$  extended in the  $(-\infty, +\infty)$  range. Using the Bloch theorem, one can restrict to  $2\pi$  periodic functions, at the (cheap) price of including a constant quasi-momentum.

The dynamics of this quasiperiodic kicked rotor is *identical* to the time-evolution of a 3D-kicked rotor:

$$H_3 = \frac{p_1^2}{2} + \omega_2 p_2 + \omega_3 p_3 + K \cos \theta_1 [1 + \varepsilon \cos \theta_2 \cos \theta_3] \sum_n \delta(t - n), \quad (3)$$

with an initial condition:

$$\Psi_3(\theta_1, \theta_2, \theta_3, t = 0) \equiv \Psi_{qp}(\theta_1, t = 0) \delta(\theta_2 - \varphi_2) \delta(\theta_3 - \varphi_3). \quad (4)$$

where  $\Psi_{qp}(\theta, t = 0)$  is an arbitrary initial condition for the quasiperiodic kicked rotor. Note that dynamical localization takes place in momentum and not in configuration space. The initial state being perfectly localized in  $\theta_2$  and  $\theta_3$ , it is entirely delocalized in the conjugate momenta  $p_2$  and  $p_3$  so that we will study transport along the  $p_1$  direction, which is tantamount to measure the momentum distribution of the quasiperiodic kicked rotor  $|\Psi_{qp}(p, t)|^2$ . The unusual linear dependence of  $H_3$  with  $p_2$  and  $p_3$  does not prevent, for  $\varepsilon \neq 0$  the dynamics to be similarly diffusive or localized along the 3 coordinates.

The Hamiltonian  $H_3$  is invariant under the transformation  $T : t \rightarrow -t, \theta \rightarrow -\theta, \mathbf{p} \rightarrow \mathbf{p}$ , i.e. the time reversal in the momentum representation, which is the relevant one for dynamical localization (see [22, 23]). In particular, the choice of a non-zero quasi-momentum and non-zero phases  $\varphi_2$  or  $\varphi_3$  does not break time reversal symmetry.

The evolution of the states according to Hamiltonian (1) is governed by the operator  $U$  (see below, Eq. (5)), belonging to the Circular Orthogonal Ensemble class [24], with the additional constraint (4) at  $t = 0$ ; this shows that the dynamical properties of the present quasiperiodic kicked rotor also belong to the orthogonal ensemble.

It should also be noted that the 3D aspect comes from the fact that 3 frequencies are present in our dynamical system: the usual “momentum frequency”  $\hbar$  which is present in the standard kicked rotor (with  $\varepsilon = 0$ ), and the two additional time-frequencies  $\omega_2$  and  $\omega_3$ . By increasing the number of incommensurate frequencies, one should be able to tune the effective dimensionality of the system. This holds the promise of extending the study of the Anderson transition to higher dimensions.

From a stroboscopic point of view, the quantum dynamics of the 3D-kicked rotor Eq. (3) is determined by its evolution operator over one period:

$$U = e^{-iK \cos \theta_1 (1 + \varepsilon \cos \theta_2 \cos \theta_3) / \hbar} \times e^{-i(p_1^2/2 + \omega_2 p_2 + \omega_3 p_3) / \hbar}, \quad (5)$$

whose eigenstates form a basis set allowing to calculate the temporal evolution. These Floquet states  $|\phi\rangle$  are fully characterized by their quasienergy  $\omega$ , defined modulo  $2\pi$ :

$$U|\phi_\omega\rangle = e^{-i\omega}|\phi_\omega\rangle. \quad (6)$$

Equivalence with a 3D-Anderson tight-binding model can be obtained by reformulating Eq. (6) for the Floquet states [2]:

$$\epsilon_{\mathbf{m}} \Phi_{\mathbf{m}} + \sum_{\mathbf{r} \neq 0} W_{\mathbf{r}} \Phi_{\mathbf{m}-\mathbf{r}} = -W_{\mathbf{0}} \Phi_{\mathbf{m}}, \quad (7)$$

where  $\mathbf{m} \equiv (m_1, m_2, m_3)$  and  $\mathbf{r}$  label sites on a 3D lattice, and the  $\Phi_{\mathbf{m}}$  are simply related to the Fourier components of the Floquet state  $|\phi_\omega\rangle$ . The on-site energy  $\epsilon_{\mathbf{m}}$  reads:

$$\epsilon_{\mathbf{m}} = \tan \left\{ \frac{1}{2} \left[ \omega - \left( \hbar \frac{m_1^2}{2} + \omega_2 m_2 + \omega_3 m_3 \right) \right] \right\}, \quad (8)$$

and the hopping amplitudes  $W_{\mathbf{r}}$  are coefficients of a threefold Fourier expansion of  $W(\theta) = \tan [K \cos \theta_1 (1 + \varepsilon \cos \theta_2 \cos \theta_3) / 2\hbar]$ .

When  $(\hbar, \omega_2, \omega_3, 2\pi)$  is an incommensurate quadruplet, the classical dynamics can become chaotic (for sufficiently large stochasticity parameter  $K \gtrsim 2$ ) with diffusive spreading in *all*  $\mathbf{m}$  directions [15]. The pseudo-random character of the potential  $\epsilon_{\mathbf{m}}$  then gives the disorder in the model (7). This pseudo-random disorder is not  $\delta$ -correlated, which implies that the quasiperiodic kicked rotor is not identical to the Anderson model. It is known that long-range potential correlations may affect in various ways (including destroy the localization) the Anderson localization [25, 26]; however, in our system, these long-range correlations are absent.

We therefore expect to observe localization effects as predicted for the standard 3D-Anderson model. Localized

states would be observed if the disorder strength is large as compared to the hopping amplitudes. In the case of model (7), while the amplitude of disorder is fixed, the hopping amplitudes increase with  $K$ . Therefore, for large  $K$  a diffusive regime should be observed, while for small  $K$  (though sufficiently large as to prevent classical localization effects) a localized regime is expected. This was validated both numerically [15] and experimentally [16].

**Finite-time scaling.** – In the case of the kicked rotor, the initial classical chaotic diffusion is stopped only after a certain characteristic time, the localization time  $\tau_\ell$  which turns out to be roughly proportional to the localization “length” (characterizing the exponential localization in momentum space) [27]:  $\tau_\ell \propto \ell$ . In 3D, the localization time scales as  $\tau_\ell \sim \ell^3$ . Thus for very large localization length,  $\tau_\ell$  may exceed the largest time accessible (the maximum duration of a cold-atoms experiment is typically 150 kicks [16] whereas numerical investigations can go up to  $10^6$  kicks). Consequently, it is vain to investigate the Anderson transition only from static properties of the quasiperiodic kicked rotor, such as the divergence of the localization length at criticality, which could be obtained only for  $t \gg \tau_\ell$ . Note however that some useful information can be extracted from the statistical properties of the energy levels (the Floquet quasi-energies in our specific case of a kicked system), which display marked changes at the transitions [24, 26, 28].

Actually, these finite-time effects are similar to finite-size effects for the study of classical or quantum phase transitions. We can generalize the usual scaling laws to cover our time-dependent problem. The single parameter scaling theory, successfully used for the standard (static) 3D Anderson model [29–31], can be applied to analyze the dynamics (see [16]) and especially to determine the critical properties of the Anderson transition, i.e. the critical exponents.

The dynamics of the quasiperiodic kicked rotor is conveniently studied by considering the time-evolution of the variance of the momentum distribution  $\langle p^2 \rangle$ , the average being taken over several initial conditions, which corresponds to an average over disorder. We can make the following scaling hypothesis for this quantity [32]:

$$\langle p^2 \rangle = t^{k_1} F[(K - K_c) t^{k_2}] , \quad (9)$$

with  $F$  a function characteristic of the transition (to be determined) and  $k_1$  and  $k_2$  two exponents which can be constrained as explained in the following.  $K_c$  is the critical value of the stochasticity parameter. We must recover as  $t \rightarrow \infty$  either a diffusive behavior  $\langle p^2 \rangle \sim Dt$  when  $K > K_c$  or a localized dynamics  $\langle p^2 \rangle \sim \ell^2$  when  $K < K_c$ . In the vicinity of the transition, the diffusion constant  $D \sim (K - K_c)^s$  vanishes with the critical exponent  $s$  and the localization length  $\ell \sim (K_c - K)^{-\nu}$  diverges with the critical exponent  $\nu$ . The Wegner’s law [33]  $s = \nu$  in three dimensions, then leads to  $k_1 = 2/3$  and  $k_2 = 1/3\nu$  [34].

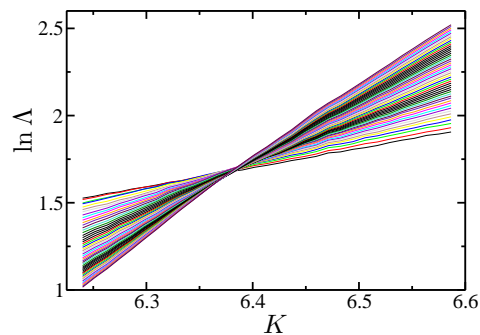


Fig. 1: (Color online) Dynamics of the quasiperiodic kicked rotor in the vicinity of the critical regime. The rescaled quantity  $\ln \Lambda(K, t)$  is plotted as a function of  $K$  for various values of time  $t$  ranging from  $t = 30$  to  $t = 40000$ . The crossing of the different curves at a common point ( $K_c \simeq 6.4$ ,  $\ln \Lambda_c \simeq 1.6$ ) indicates the occurrence of the metal-insulator transition. The parameters are that of the set  $\mathcal{A}$  (see Table 1).

Therefore, to analyze the scaling of the dynamics, the behavior of the quantity  $\Lambda = \langle (p/k)^2 \rangle t^{-2/3}$  should be investigated as a function of time and for various stochasticity parameters. Such a study was undertaken in [16] and allowed for a successful experimental characterization of the Anderson transition. In order to tackle the problem of universality of the critical behavior, we have to go one step further and study whether the critical exponent  $\nu$  changes when parameters such as  $\hbar, \omega_2, \omega_3$  are modified.

The following discussion is rather intricate but cannot be avoided in a rigorous study. Indeed, to reliably distinguish the different universality classes of the Anderson transition requires a very precise determination of the critical exponent; for instance, the value  $\nu = 1.43 \pm 0.04$  for the unitary symmetry class is very close to the one for the orthogonal symmetry class [19]. For a very accurate determination of  $\nu$ , possible systematic deviations to one-parameter scaling must be taken into account.

**Systematic corrections to scaling.** – Let us consider the scaling function  $\mathcal{F} \equiv \ln(F/k^2)$  in the vicinity of the critical point:

$$\ln \Lambda = \mathcal{F} \left[ (K - K_c) t^{1/3\nu} \right] . \quad (10)$$

One simple feature of the scaling hypothesis Eq. (10) is that when  $\ln \Lambda$  is plotted against  $K$ , the curves for different times  $t$  should intersect at the common point  $(K_c, \ln \Lambda_c = \mathcal{F}(0))$ ; this crossing, which indicates the occurrence of the metal-insulator transition, is clearly visible in Fig. 1.

In practice, the data do not exactly follow Eq. (10). There are small systematic deviations to scaling. Here, we consider several ways in which such corrections can arise (see below for a detailed discussion of each correction): (i) the presence of an irrelevant scaling variable, (ii) non-linear dependence of the scaling variables in the stochasticity parameter  $K$  and (iii) resonances due to the

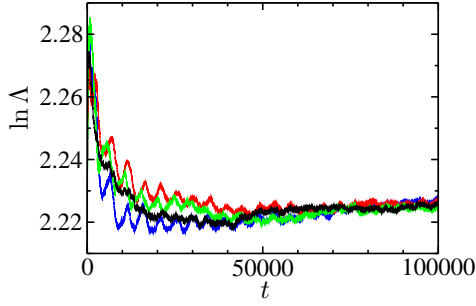


Fig. 2: (Color online) Small oscillating corrections to the scaling behavior in the critical regime. The parameters are the following:  $\tilde{k} = 2.89$ ,  $\omega_2 = 2\pi\sqrt{5}$ ,  $\omega_3 = 2\pi\sqrt{13}$ ,  $K = 7.8$  and  $\varepsilon = 0.3$ . Color curves correspond to various choices of the phases  $\varphi_2$  and  $\varphi_3$  [see Eq. (1)] whereas the black curve results from a statistical average over different phases. The amplitudes of the quasi-resonant oscillations decrease as time goes on. Averaging over the phases kills the rapidly oscillating structures, while keeping all of the other dynamical properties unchanged.

periods being well approximated by a ratio of small integers. (iii) is specific to our three-frequency dynamical system, but (i) and (ii) were shown to play an important role in the standard Anderson model [17]. Note that the most important correction to scaling is a time dependence of  $\ln \Lambda$  at  $K = K_c$  either due to (i) or (iii).

The well-known deviations (i) and (ii) can be taken into account by adding extra terms to (10) [17]. (i) The scaling function  $\mathcal{F}$  depends not only on the relevant scaling variable  $\chi_r$  (i.e. a function of  $K - K_c$ ), but also on an irrelevant scaling variable  $\psi$ :

$$\ln \Lambda = \mathcal{F} \left( \chi_r t^{1/3\nu}, \psi t^{-y} \right). \quad (11)$$

Since  $\psi$  is an irrelevant scaling parameter, its effects should vanish as  $t$  goes to infinity, thus  $y$  must be positive. (ii) Non-linearity in the relevant scaling variable  $\chi_r$  can be described by an expansion in terms  $K - K_c$  up to order  $m_R$ .

To define a fitting function  $\mathcal{F}_f$ , we can then make a Taylor expansion of the scaling function  $\mathcal{F}$  up to order  $n_R$  in  $\chi_r t^{1/3\nu}$  and  $n_I$  in  $\psi t^{-y}$ :

$$\mathcal{F}_f(K, t) = \sum_{m=0}^{n_R} \sum_{n=0}^{n_I} \chi_r^m t^{m/3\nu} \psi^n t^{-ny} \mathcal{F}_{m,n}. \quad (12)$$

We now discuss the qualitative nature of the correction due to the presence of an irrelevant scaling variable (i) as compared to the effect of resonances (iii). In case (i),  $\ln \Lambda_c = \ln \Lambda(K = K_c)$  will shift in a monotonous way as time increases and converge to its thermodynamic limit  $\ln \Lambda_c(t = \infty)$  [ $\ln \Lambda_c(t) = \mathcal{F}_{0,0} + t^{-y} \mathcal{F}_{0,1}$  in the linear regime ( $m_R = n_R = n_I = 1$ )]. In the case of our three-frequency dynamical system, the data do not always fit such a monotonous evolution model for  $\ln \Lambda_c(t)$ . Indeed, for a generic choice of incommensurate periods, the data

are found to oscillate around their transient anomalous diffusive dynamics, see Fig. 2.

We infer that such an oscillating correction to scaling arises in a resonant way: when the frequencies can be approximately related by a simple linear combination (i.e. involving small integers), a resonance occurs. This is a rather common phenomenon in multi-frequency dynamical systems. The phase and the amplitude of the oscillations in Fig. 2 depend on the choice of the phases  $\varphi_2$  and  $\varphi_3$  of the time-modulation [see Eq. (2)], i.e. on the initial state in Eq. (4). From the point of view of the Anderson-like model Eq. (7), resonances can be interpreted as correlations in the disordered potential. Hence, to perform the standard scaling analysis devised for the Anderson model with uncorrelated disorder [17], we shall retain data only for sufficiently long times (say  $t \geq 1000$ ) and average over different initial conditions, i.e. different quasi-momenta and phases  $\varphi_2$  and  $\varphi_3$ .

We computed  $\ln \Lambda$  for times up to  $t = 10^6$  kicks with an accuracy of 0.15%. To achieve this accuracy more than 1000 initial conditions are required. To analyze data over the full range of times  $t \in [10^3, 10^6]$ , we fit the model Eq. (12) to the data. Note that the inclusion of the corrections (i) and (ii) in Eq. (12) leads to a rapid increase in the number of fitting parameters. That is why high quality data with a wide range of variation of  $t^{1/3}$  are needed if meaningful fits are to be obtained.

The most likely fit is determined by minimizing the  $\chi^2$  statistics measuring the deviation, due to the numerical uncertainties, between the model and data. Some typical numerical data and the associated fit are displayed in Fig. 3. To exhibit scaling, we subtract the corrections due to the irrelevant scaling variable [17] obtaining the corrected quantity  $\ln \Lambda_s$ . As seen in Fig. 4, all data collapse almost perfectly on the scaling function deduced from the model  $\mathcal{F}_f$ .

No significant deviation of the scaling function from the fit is observed. The goodness of fit  $Q$  has been determined using the  $\chi^2$  distribution with  $N_d - N_p$  degrees of freedom where  $N_d$  is the total number of data we used to fit the model and  $N_p$  is the total number of fitting parameters (see Table 1). The confidence intervals (one standard deviation) for the fitted parameters were estimated using the bootstrap method which yields Monte Carlo estimates of the errors in the fitted parameters.

**Universality.** – A key property of the Anderson transition is that it is a continuous (i.e. second order) phase transition whose critical behavior can be described in a framework of universality classes [5]. This means that the critical exponents should not be sensitive to the microscopic details of the disordered potential but should depend only on the underlying symmetries (e.g. time reversal symmetry). We present here new material that allows us to numerically prove that this is indeed the case for the quasiperiodic kicked rotor, thus strengthening the fact that this system is in the same universality class than the

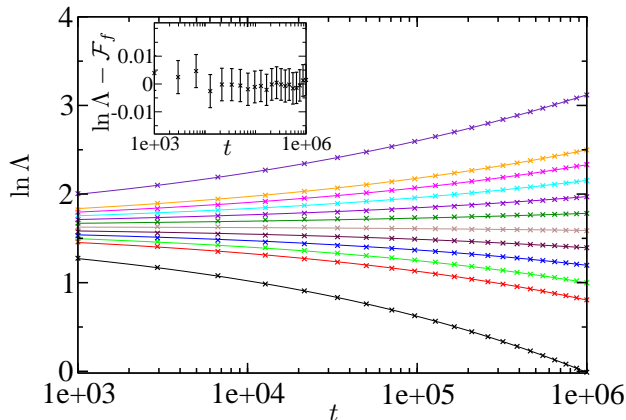


Fig. 3: (Color online)  $\ln \Lambda$  as a function of time  $t$ . The **curves** are fits of the data according to the model  $\mathcal{F}_f$  [see Eq. (12)] with  $n_R = 3$ ,  $m_R = 2$ ,  $n_I = 1$ . The parameters are that of the set  $\mathcal{D}$  (see Table 1). The inset shows the deviations of the data (corresponding to  $K = 7.9$ ) to the most likely fit, showing no statistically significant deviation.

truly random Anderson transition.

We have carried on a *detailed* study of four cases characterized by different set of parameters, see Table 1):  $\mathcal{A}$  and  $\mathcal{B}$  are both optimal set of parameters for experimental studies (see [16]), while  $\mathcal{C}$  and  $\mathcal{D}$  are rather for theoretical/numerical considerations.  $\mathcal{C}$  is a first step towards an ideal choice of parameters:  $\omega_2/\omega_3 = \eta$  where  $\eta$  is the silver number (see below), and the continuous fraction of  $\bar{k}/\pi$  is constituted of small integers (to prevent the system to be close to a resonance).  $\mathcal{D}$  should be a “best choice” of parameters if we seek the least correlations in the disorder Eq. (8). It is such that  $\bar{k}$ ,  $\omega_2$ ,  $\omega_3$  and  $\pi$  are a “most incommensurate” *quadruplet* of numbers. As suggested in [14], we set  $\bar{k} = \alpha$ ,  $\omega_2 = \alpha/\eta$  and  $\omega_3 = \alpha/\eta^2$  where  $\eta = 1.324717\dots$  (the silver number which generalizes the golden number for triplet instead of pair of incommensurate numbers [35]) is the real root of the equation  $\eta^3 - \eta - 1 = 0$ , and  $\alpha = 3.5399\dots$  is such that the continuous fractions of  $\bar{k}/\pi = \alpha/\pi$ ,  $\omega_2/\pi = \alpha/\eta\pi$  and  $\omega_3/\pi = \alpha/\eta^2\pi$  are constituted of small ( $< 9$ ) integers.

The details of the simulations and the types of fit used to analyze those sets are listed in Table 2. The estimated critical parameters and their confidence intervals are given in Table 3. Some *typical* data and scaling function are drawn in Figs. 3 and 4.

The most important conclusion to be drawn from Table 3 is that the estimates of the exponent  $\nu$  for the four different sets are in almost perfect agreement with each other and with the estimate of  $\nu$  based on numerical studies of the truly random Anderson model  $\nu = 1.57 \pm 0.02$  of the orthogonal symmetry class [17]. Note also that in the case of the quasiperiodic kicked rotor, the critical stochasticity  $K_c$  and  $\ln \Lambda_c$  depend on: (i) the anisotropy governed by the parameter  $\epsilon$  and (ii)  $\bar{k}$ ,  $\omega_2$  and  $\omega_3$ . The dependence

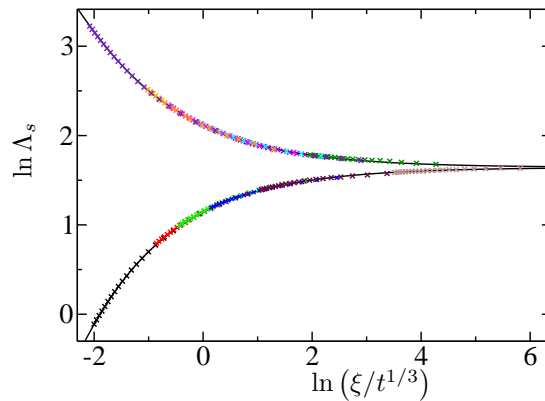


Fig. 4: (Color online)  $\ln \Lambda_s$ , the data in Fig. 3 after subtraction of corrections due to the irrelevant scaling variable, plotted versus  $\ln(\xi/t^{1/3})$  where  $\xi = |\chi_r|^{-\nu}$  and the scaling function deduced from the model  $\mathcal{F}_f$ , Eq. (12) (black curve). The parameters are that of the set  $\mathcal{D}$  (see Table 1). The best fit estimates of the critical stochasticity and the critical exponent are:  $K_c = 8.09 \pm 0.01$ ,  $\ln \Lambda_c = 1.64 \pm 0.03$  and  $\nu = 1.59 \pm 0.01$ .

(i) of the critical disorder and critical  $\ln \Lambda$  on anisotropy is a typical feature of the Anderson transition in anisotropic solids [20]. The dependence (ii) follows from the relation between the initial “classical” diffusion constant and the parameters  $\bar{k}$ ,  $\omega_2$  and  $\omega_3$  [27].

The Anderson transition with the quasiperiodic kicked rotor is a robust feature: indeed, the “naive” choices of parameters, set  $\mathcal{A}$  and  $\mathcal{B}$ , lead to very clean critical behaviors, as clean as for the sophisticated choices of parameters, sets  $\mathcal{C}$  and  $\mathcal{D}$ . Our experience is that for certain mutually incommensurate triplets  $(\bar{k}, \omega_2, \omega_3)$  systematic deviations to scaling (such as resonances) can occur for intermediate times, but eventually vanish.

**Conclusion.** – A numerical analysis of the critical behavior of the quasiperiodic kicked rotor has shown that this quantum-chaotic system exhibits the same critical phenomena as the truly random Anderson model, i.e. both systems belong to the same (orthogonal) universality class [21]. By taking proper account of corrections to the scaling property around criticality, the universality of the critical exponent  $\nu$  for the quasiperiodic kicked rotor was demonstrated. The critical exponent  $\nu$  was determined with an accuracy better or comparable to the one achieved in previous numerical studies of the 3D-Anderson model [17, 19, 20]. Our result  $\nu = 1.59 \pm 0.01$  is in perfect agreement with the value found for the orthogonal symmetry class [17]. It is clearly distinct from the value found for the unitary class  $\nu = 1.43 \pm 0.04$  [19], and from the predictions  $\nu = 1$  of the self-consistent theory of localization [37] and  $\nu = 1.5$  of a recent *ad hoc* refinement of the self-consistent theory [38].

\*\*\*

We thank J.C. Garreau, P. Szriftgiser, J. Chabé, H. Lig-

	$\tilde{k}$	$\omega_2$	$\omega_3$	$K$	$\epsilon$
$\mathcal{A}$	2.85	$2\pi\sqrt{5}$	$2\pi\sqrt{13}$	6.24 → 6.58	0.413 → 0.462
$\mathcal{B}$	2.85	$2\pi\sqrt{7}$	$2\pi\sqrt{17}$	5.49 → 5.57	0.499 → 0.514
$\mathcal{C}$	2.2516	$1/\eta$	$1/\eta^2$	4.98 → 5.05	0.423 → 0.436
$\mathcal{D}$	3.5399	$\tilde{k}/\eta$	$\tilde{k}/\eta^2$	7.9 → 8.3	0.425 → 0.485

Table 1: The four sets of parameters considered:  $\tilde{k}$ ,  $\omega_2$  and  $\omega_3$  control the microscopic details of the disorder, while  $\epsilon$  drives the anisotropy of the hopping amplitudes. In  $\mathcal{C}$ ,  $\omega_2/\omega_3 = \eta$  where  $\eta$  is the silver number (see below), and the continuous fraction of  $\tilde{k}/\pi$  is constituted of small integers.  $\mathcal{D}$  is such that  $\tilde{k} = \alpha$ ,  $\omega_2 = \alpha/\eta$  and  $\omega_3 = \alpha/\eta^2$  where  $\eta = 1.324717\dots$  the real root of the equation  $\eta^3 - \eta - 1 = 0$ , and  $\alpha$  is such that the continuous fractions of  $\tilde{k}/\pi = \alpha/\pi$ ,  $\omega_2/\pi = \alpha/\eta\pi$  and  $\omega_3/\pi = \alpha/\eta^2\pi$  are constituted of small ( $< 9$ ) integers [35].

nier and F. Farago for many interesting and fruitful discussions.

## REFERENCES

- [1] ANDERSON P. W., *Phys. Rev.*, **109** (1958) 1492.
- [2] FISHMAN S., GREMPEL D. R. and PRANGE R. E., *Phys. Rev. Lett.*, **49** (1982) 509.
- [3] CASATI G., GUARNERI I., IZRAILEV F. and SCHARF R., *Phys. Rev. Lett.*, **64** (1990) 5.
- [4] FYODOROV Y. V. and MIRLIN A. D., *Phys. Rev. Lett.*, **67** (1991) 2405.
- [5] EFETOV K., *Supersymmetry in Disorder and Chaos* (Cambridge University Press, Cambridge, UK) 1997.
- [6] ALTLAND A. and ZIRNBAUER M. R., *Phys. Rev. Lett.*, **77** (1996) 4536.
- [7] JANSSEN M., *Physics Reports*, **295** (1998) 1.
- [8] HEFEI H., STRYBULEVYCH A., PAGE J. H., SKIPETROV S. E. and VAN TIGGELEN B. A., *Nat. Phys.*, **4** (2008) 945.
- [9] CHABANOV A. A., STOYTCHEV M. and GENACK A. Z., *Nature (London)*, **404** (2000) 850.
- [10] WIERSMA D. S., BARTOLINI P., LAGENDIJK A. and RIGHINI R., *Nature (London)*, **390** (1997) 671.
- [11] STÖRZER M., GROSS P., AEGERTER C. M. and MARET G., *Phys. Rev. Lett.*, **96** (2006) 063904.
- [12] SCHWARTZ T., BARTAL G., FISHMAN S. and SEGEV B., *Nature (London)*, **446** (2007) 52.
- [13] MOORE F. L., ROBINSON J. C., BHARUCHA C., WILLIAMS P. E. and RAIZEN M. G., *Phys. Rev. Lett.*, **73** (1994) 2974.
- [14] WANG J. and GARCÍA-GARCÍA A. M., *Phys. Rev. E*, **79** (2009) 036206.
- [15] CASATI G., GUARNERI I. and SHEPELYANSKY D. L., *Phys. Rev. Lett.*, **62** (1989) 345.
- [16] CHABÉ J., LEMARIÉ G., GRÉMAUD B., DELANDE D., SZRIFTGISER P. and GARREAU J. C., *Phys. Rev. Lett.*, **101** (2008) 255702.
- [17] SLEVIN K. and OHTSUKI T., *Phys. Rev. Lett.*, **82** (1999) 382.
- [18] BASKO D. M., SKVORTSOV M. A. and KRAVTSOV V. E., *Phys. Rev. Lett.*, **90** (2003) 096801.
- [19] SLEVIN K. and OHTSUKI T., *Phys. Rev. Lett.*, **78** (1997) 4083.
- [20] MILDE F., RÖMER R., SCHREIBER M. and V. U., *Eur. Phys. J. B*, **15** (2000) 685.
- [21] EVERS F. and MIRLIN A. D., *Rev. Mod. Phys.*, **80** (2008) 1355.
- [22] SCHARF R., *J. Phys. A*, **22** (1989) 4223.
- [23] BLÜMEL R. and SMILANSKY U., *Phys. Rev. Lett.*, **69** (1992) 217.
- [24] GARCÍA-GARCÍA A. M. and WANG J., *Acta Phys. Pol. A*, **112** (2007) 635.
- [25] TESSIERI L., *J. Phys. A: Math. Gen.*, **35** (2002) 9585.
- [26] CARPENA P., BERNAOLA-GALVÁN P. and IVANOV P. CH., *Phys. Rev. Lett.*, **93** (2004) 176804.
- [27] SHEPELYANSKY D. L., *Phys. Rev. Lett.*, **56** (1986) 677.
- [28] LEMARIÉ G. ET AL, *unpublished*, (2009).
- [29] ABRAHAMS E., ANDERSON P. W., LICCIARDELLO D. C. and RAMAKRISHNAN T. V., *Phys. Rev. Lett.*, **42** (1979) 673.
- [30] MACKINNON A. and KRAMER B., *Phys. Rev. Lett.*, **47** (1981) 1546.
- [31] PICHARD J. L. and SARMA G., *J. Phys. C*, **14** (1981) L127.
- [32] STAUFFER D. and AHARONY A., *Introduction to Percolation Theory* 2nd Edition (Taylor and Francis) 1994.
- [33] WEGNER F., *Z. Phys. B*, **25** (1976) 327.
- [34] OHTSUKI T. and KAWARABAYASHI T., *J. Phys. Soc. Jpn.*, **66** (1997) 314.
- [35] KIM S.-H. and OSTLUND S., *Phys. Rev. A*, **34** (1986) 3426.
- [36] PANAGIOTIDES N. A., EVANGELOU S. N. and THEODOROU G., *Phys. Rev. B*, **49** (1994) 14122.
- [37] VOLLHARDT D. and WÖLFLE P., *Phys. Rev. Lett.*, **48** (1982) 699.
- [38] GARCÍA-GARCÍA A. M., *Phys. Rev. Lett.*, **100** (2008) 076404.

	$n_R$	$n_I$	$m_R$	$N_d$	$N_p$	$\chi_r^2$	$Q$
$\mathcal{A}$	3	1	2	800	12	236	1
$\mathcal{B}$	2	1	1	600	9	278	1
$\mathcal{C}$	2	1	1	1000	9	934	0.9
$\mathcal{D}$	3	1	2	1212	12	917	0.999

Table 2: Parameters used for the four sets of data: type of fit [see Eq. (12)], number of data points  $N_d$ , number of parameters  $N_p$ , value of  $\chi_r^2$  for the best fit and goodness of fit  $Q$ . Time ranges from  $t = 10^3$  to  $t = 10^6$ .

	$K_c$	$\ln \Lambda_c$	$\nu$	$y$
$\mathcal{A}$	$6.36 \pm 0.02$	$1.60 \pm 0.04$	<b><math>1.58 \pm 0.01</math></b>	$0.71 \pm 0.28$
$\mathcal{B}$	$5.53 \pm 0.03$	$1.08 \pm 0.09$	<b><math>1.60 \pm 0.03</math></b>	$0.33 \pm 0.30$
$\mathcal{C}$	$5.00 \pm 0.03$	$1.19 \pm 0.15$	<b><math>1.60 \pm 0.02</math></b>	$0.23 \pm 0.29$
$\mathcal{D}$	$8.09 \pm 0.01$	$1.64 \pm 0.03$	<b><math>1.59 \pm 0.01</math></b>	$0.43 \pm 0.23$

Table 3: Best fit estimates of the critical parameters  $K_c$  and  $\ln \Lambda_c$ , the critical exponent  $\nu$  together with their uncertainty (one standard deviation).  $\nu$  is expected to be universal whereas  $\ln \Lambda_c$  and  $K_c$  do depend on anisotropy [36] and  $\tilde{k}$ ,  $\omega_2$  and  $\omega_3$ . Irrelevant parameters are sensitive to microscopic details, therefore  $y$  is strictly positive and not universal.